

## NMR Spectroscopy

International Edition: DOI: 10.1002/anie.201904057  
German Edition: DOI: 10.1002/ange.201904057Novel  $^{13}\text{C}$ -detected NMR Experiments for the Precise Detection of RNA Structure

Robbin Schnieders, Antje C. Wolter, Christian Richter, Jens Wöhnert, Harald Schwalbe,\* and Boris Fürtig\*

**Abstract:** Up to now, NMR spectroscopic investigations of RNA have utilized imino proton resonances as reporters for base pairing and RNA structure. The nucleobase amino groups are often neglected, since most of their resonances are broadened beyond detection due to rotational motion around the C–NH<sub>2</sub> bond. Here, we present  $^{13}\text{C}$ -detected NMR experiments for the characterization of all RNA amino groups irrespective of their motional behavior. We have developed a C(N)H-HDQC experiment that enables the observation of a complete set of sharp amino resonances through the detection of proton-NH<sub>2</sub> double quantum coherences. Further, we present an “amino”-NOESY experiment to detect NOEs to amino protons, which are undetectable by any other conventional NOESY experiment. Together, these experiments allow the exploration of additional chemical shift information and inter-residual proton distances important for high-resolution RNA secondary and tertiary structure determination.

Amino groups are important functional groups in the nucleobases of DNA and RNA. Due to their hydrogen bonding potential they are directly involved in stabilizing Watson–Crick and many other base pairing interactions.<sup>[1]</sup> They also mediate RNA–protein and RNA–ligand interactions.<sup>[2]</sup> Despite their functional relevance, structural and chemical shift information for amino groups is very limited. The NMR signals of amino groups are difficult to detect in conventional NMR experiments since their proton resonances usually exhibit large line widths. Especially for guanosines and adenosines, normally only a small fraction of the expected

signals is observed in conventional  $^{15}\text{N}$ -HSQC-spectra. As a consequence, assignment information for RNA amino groups is scarce in the BMRB database.<sup>[3]</sup> Overall, NMR signal assignments are available for only approximately 20% of all purine amino groups and for approximately 60% of all cytidine amino groups. Furthermore, missing signal assignments or the lack of observable amino proton signals severely limits the collection of NOE or hydrogen bond restraints involving nucleobase amino groups.

The line broadening of the proton signals of amino groups is caused by exchange due to the restricted rotation around the C–NH<sub>2</sub> bond with rates of approximately  $k_{\text{rot-CN}}^{\text{A}} \approx 400\text{--}6500\text{ s}^{-1}$ <sup>[4]</sup> and  $k_{\text{rot-CN}}^{\text{G}} \approx 200\text{--}1100\text{ s}^{-1}$ .<sup>[5]</sup> In contrast, for amino groups in cytidines, the rotation rate at ambient temperature is considerably slower with  $k_{\text{rot-CN}}^{\text{C}} \approx 40\text{ s}^{-1}$ .<sup>[6]</sup> As the rates for amino groups in guanosines and adenosines match the difference in chemical shift of the amino group protons, their NMR signals are in intermediate exchange and consequently broadened beyond detectability.<sup>[4,5]</sup> In order to minimize losses due to exchange, CPMG-based transfers are utilized in some NMR pulse sequences that correlate amino protons to adjacent nitrogens.<sup>[7]</sup> However, even then only a subset of the expected resonances can be observed at room temperature.<sup>[8]</sup>

In contrast to the protons of the amino group, its nitrogen atom exhibits a narrow NMR line shape. It can be easily correlated with adjacent carbon atoms due to sizeable scalar couplings ( $J_{\text{CN}} = 20\text{--}23\text{ Hz}$ ). Therefore, the nitrogen atom can be observed in NMR experiments utilizing carbon detection.<sup>[9]</sup>

Here, we present a suite of NMR experiments allowing identification and structural characterization of RNA amino groups even in the presence of severe exchange broadening. We introduce a  $^{13}\text{C}$ -detected C(N)H-HDQC experiment, which evolves double quantum (DQ) proton magnetization in the indirect dimension and therefore enables the detection of sharp signals for all amino resonances independent of their barrier to rotation. A conceptually similar approach was recently successfully applied in the development of an  $\text{N}_{\eta}$ -DQ experiment for arginine residues in proteins.<sup>[10]</sup>

Furthermore, we have developed a  $^{13}\text{C}$ -detected “amino”-NOESY experiment in which NOE contacts to the NH<sub>2</sub>-groups can be observed, which are not detectable in conventional NOESY experiments.

In the following, we discuss the path of magnetization transfer for both of the experiments (Figure 1 and Supporting Information, Figure S1). In the  $^{13}\text{C}$ -detected C(N)H-HDQC experiment, carbon nuclei are excited and the magnetization is selectively transferred to the amino nitrogen via an INEPT-

[\*] R. Schnieders, Dr. C. Richter, Prof. Dr. H. Schwalbe, Dr. B. Fürtig  
Institute for Organic Chemistry and Chemical Biology,  
Center for Biomolecular Magnetic Resonance (BMRZ),  
Johann Wolfgang Goethe-Universität Frankfurt  
Max-von-Laue-Str. 7, 60438 Frankfurt (Germany)  
E-mail: schwalbe@nmr.uni-frankfurt.de  
fuertig@nmr.uni-frankfurt.de

A. C. Wolter, Prof. Dr. J. Wöhnert  
Institute for Molecular Biosciences,  
Center for Biomolecular Magnetic Resonance (BMRZ),  
Johann Wolfgang Goethe-Universität Frankfurt  
Max-von-Laue-Str. 9, 60438 Frankfurt (Germany)

Supporting information and the ORCID identification number(s) for the author(s) of this article can be found under:  
<https://doi.org/10.1002/anie.201904057>.

© 2019 The Authors. Published by Wiley-VCH Verlag GmbH & Co. KGaA. This is an open access article under the terms of the Creative Commons Attribution Non-Commercial NoDerivs License, which permits use and distribution in any medium, provided the original work is properly cited, the use is non-commercial and no modifications or adaptations are made.

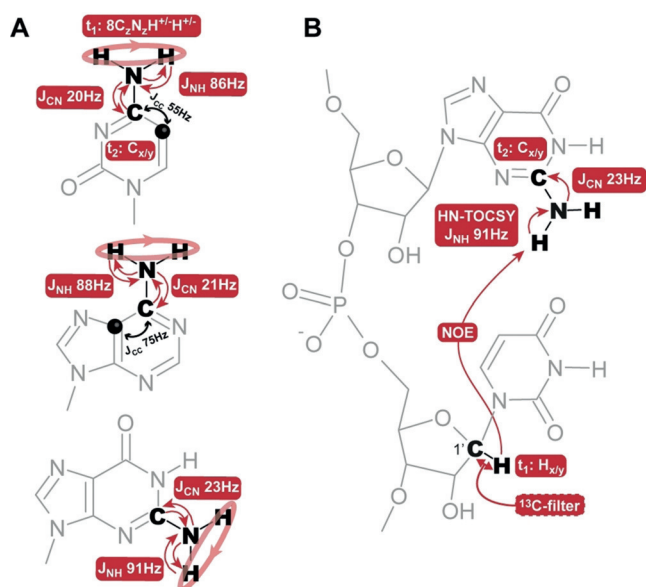


**Figure 1.** Coherence transfer pathways for the C(N)H-HDQC experiment (A) and for the "amino"-NOESY experiment with optional  $^{13}C$ -filter (B). The scalar coupling constants relevant for the appropriate magnetization transfers and the detected coherences are annotated accordingly. If not otherwise indicated, the transfer method is INEPT.<sup>[11]</sup>

step. The magnetization transfer from nitrogen to proton follows in a second INEPT-step and the last nitrogen  $90^\circ$ -pulse selects  $8C_2N_2H_2H_2$  longitudinal four-spin order. This four-spin order is then further converted into double and zero quantum coherence ( $8C_2N_2H^+/H^{+-}$ ) and the double quantum coherence is selected through phase cycling. After DQ chemical shift evolution, the coherence is transferred back via the nitrogen to carbon where it is then detected.

This experiment results in a two-dimensional C–H correlation spectrum correlating double quantum coherence of the amino group protons and SQ coherence of the carbon atom to which the amino group is covalently bound.

In the "amino"-NOESY experiment,  $^1H$   $z$ -magnetization with  $T_1$ -times of approximately 150 ms is transferred via NOE to amino protons within a distance of around 5 Å. Transfer to the adjacent nitrogen follows via hetero-TOCSY H–N transfer.<sup>[12]</sup> Ultimately, the magnetization is transferred to the adjacent carbon nucleus by an INEPT-step. The NMR signal is detected on the very sharp resonance signal of the quaternary carbon nucleus. Additionally, a  $^{13}C$ -filter can be applied before the NOESY step. This will eliminate the broad SQ diagonal amino resonances and select for NOESY signals between carbon-attached protons and  $NH_2$ -groups.

In both experiments, the last N–C INEPT-step can be replaced by an IPAP sequence<sup>[13]</sup> for homonuclear  $^{13}C$ -decoupling to eliminate the multiplet structure that arises from scalar couplings to the adjacent carbon atoms in uniformly  $^{13}C$ -labeled cytidines and adenosines (Supporting Information, Figure S1B,D).

We optimized both experiments using a 14 nt hairpin RNA containing an UUCG tetraloop<sup>[8b,14]</sup> and also applied them to the 34 nt GTP class II aptamer.<sup>[15]</sup> For comparison,

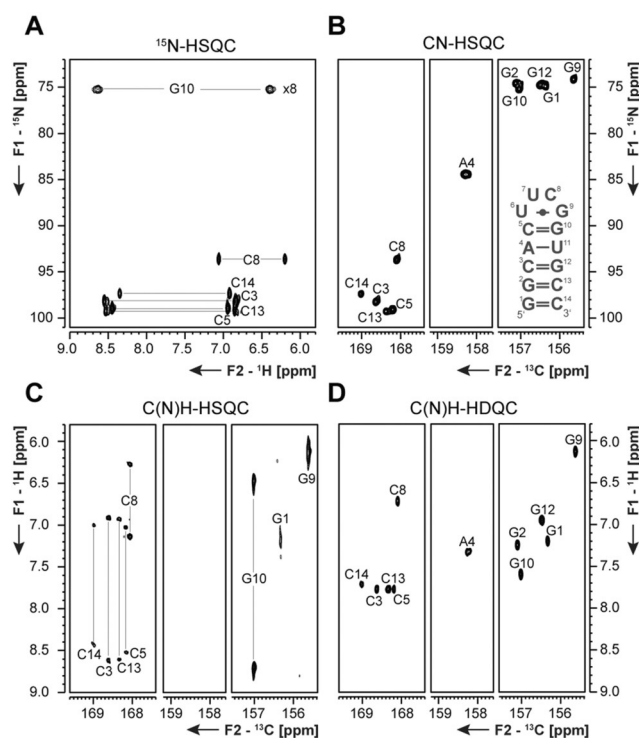


**Figure 2.** A)  $^{15}N$ -HSQC, B) CN-HSQC, C) C(N)H-HSQC, and D) C(N)H-HDQC spectra of the amino-region of the 14 nt RNA with UUCG tetraloop. The HDQC-experiment was recorded with optimized parameters for each type of nucleotide, but can also be recorded as a single experiment with averaged parameters (see Figure S2 in the Supporting Information). For experimental details, see the Supporting Information.

a set of experiments including a  $^{15}N$ -HSQC with CPMG transfer<sup>[7a]</sup> (Figure 2A), a CN-HSQC<sup>[9,16]</sup> (Figure 2B), and a C(N)H-HSQC (Figure 2C) were recorded along with the C(N)H-HDQC experiment (Figure 2D and Supporting Information, Figure S2). For the UUCG tetraloop RNA, all of the expected correlations between amino group nitrogens and adjacent carbons are observed in the CN-HSQC. In contrast, in the conventional  $^{15}N$ -HSQC spectrum, signals for the adenosine amino group and all but one (G10) of the guanosine amino groups are missing. Only for the cytidine residues a full set of  $NH_2$ -group signals is detected because CN-bond rotation for cytidine is considerably slower. In the C(N)H-HSQC experiment, additional amino group signals (G1, G9) become observable, but the amino groups of G2, G12, and A4 are still not observed. The detectability of G1 and G9 in the  $^{13}C$ -detected C(N)H-HSQC can be attributed to the fact that the proton magnetization stays along the  $z$ -axis during all INEPT-transfer steps but is transverse and therefore dephased by rotational exchange during the NH transfer in the  $^{15}N$ -HSQC.

In contrast, the C(N)H-HDQC experiment exhibits C–H correlations for all residues. Here, a single signal with a resonance frequency at the average  $^1H$  chemical shift of the two amino protons can be observed for every residue. When compared to the SQ version of the C(N)H-experiment a substantial narrowing of all signals is detected as the peak

width at half height is now independent of the C–N bond rotation rate (Supporting Information, Figure S3). A significant reduction of the signal line widths is observed for all nucleobases, but it is particularly pronounced for guanosines and adenosines.

We then applied the C(N)H-HDQC experiment to the 34 nt GTP class II aptamer that contains multiple non-canonical base pairs. The  $^{15}\text{N}$ -HSQC spectrum for this RNA shows only an incomplete set of signals for adenosine and guanosine amino groups. In the carbon-detected SQ C(N)H experiment only one additional signal for residue G1 can be detected (Supporting Information, Figure S4B), whereas signals for all amino-group-carrying residues can be detected in the new C(N)H-HDQC experiment (Figure 3). It is important to note that the DQ-experiment yields high quality spectra within a couple of hours even on spectrometers equipped with cryogenic probes optimized for  $^1\text{H}$ -detection (Supporting Information, Figure S4C).

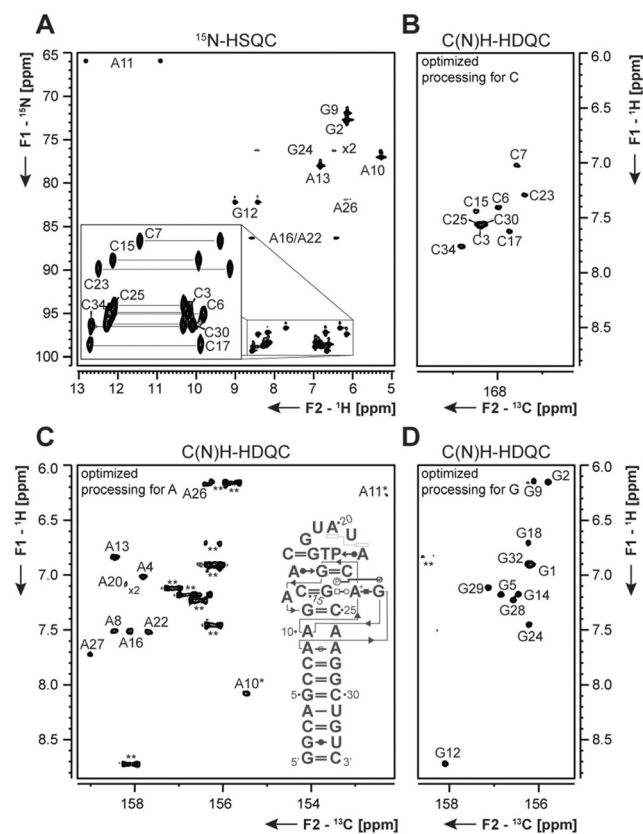


**Figure 3.** A)  $^{15}\text{N}$ -HSQC spectrum of the amino-region of the 34 nt GTP class II aptamer. B, C, and D) C(N)H-HDQC spectra for the cytidine, adenosine, and guanosine regions, respectively. Signals marked with “\*” are folded in the indirect dimension and resonances marked with “\*\*” appear in the spectrum optimized for adenosines and guanosines as pseudo doublets due to processing and arise from guanosines and adenosines, respectively. For experimental details, see the Supporting Information. C) The secondary structure of the GTP class II aptamer RNA. Arrows indicate the backbone direction (from 5' to 3'). Base pairs are displayed using the nomenclature from Leontis and Westhof.<sup>[18]</sup> The structure of the non-canonical interactions is shown in Figure S5F in the Supporting Information.

With the availability of a complete set of amino proton DQ-chemical shifts, they can be correlated with structural features of the investigated RNA (Supporting Information, Figure S5). Here, we analyzed the HDQC-experiments for five RNAs of different structural complexity, including a 329 nt long (CUG)<sub>97</sub> repeat with G-rich 5'- and 3'-overhangs.<sup>[17]</sup> A clear discrimination between canonical and non-canonical base interactions, occurring in secondary or tertiary structure elements, can be observed.

To gain detailed structural information involving amino proton resonances, we developed a carbon-detected “amino”-NOESY experiment. It correlates  $^1\text{H}$  nuclei, which are located approximately 5 Å of an amino group, with the anchoring nucleobase carbon. Applied to the reference 14 nt RNA (Supporting Information, Figure S6), the spectrum shows NOE cross signals for all three nucleotides with an exocyclic amino group. However, it is obvious that very broad amino proton diagonal signals dominate the spectrum. These signals appear at positions, where also cross-peaks to ribose H1'-protons are expected. In order to eliminate these non-informative correlations, a variant of the experiment was established, where only  $^{13}\text{C}$ -attached protons give rise to NOE cross signal (Supporting Information, Figure S6, red). Indeed, the resulting spectrum exhibits multiple amino-to-backbone correlations that have not been observed previously in conventional proton-detected NOESY experiments.

When recorded for the 34 nt GTP class II aptamer RNA (Figure 4), the  $^{13}\text{C}$ -detected NOESY experiment yields 22 new, previously unobservable NOE distance restraints. 17 of

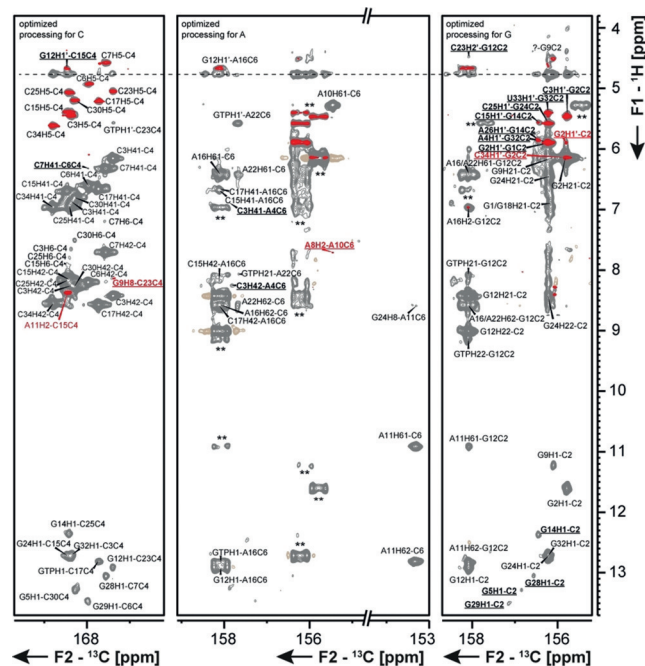


**Figure 4.** “Amino”-NOESY spectrum with (red) and without (gray)  $^{13}\text{C}$ -filter of the GTP class II aptamer. Signals marked with “\*\*” appear in the spectrum optimized for adenosines as pseudo doublets due to processing and arise from guanosines. NOE contacts, which could not be detected in  $^1\text{H}$ -based experiments, are labeled with bold and underlined letters. The water resonance is marked with a dashed line. For experimental details, see the Supporting Information.



these restraints are inter-residual correlations. Furthermore, new NOE interactions for amino groups that did not exhibit meaningful NOEs in  $^1\text{H}$ -detected spectra were identified, such as for G1 (5'-terminus), A4, G14, and G32. The majority of these NOE contacts connect amino groups to ribose H1'-protons of succeeding or cross-strand nucleotides.

The newly observed amino-group NOEs were integrated as restraints into structure calculations for the GTP class II aptamer, in addition to the previously described set of distance and torsion angle restraints.<sup>[15a]</sup> Importantly, the new restraints are fully compatible with the previously reported structure, as seen from the absence of distance violations in the newly calculated structural bundle. In this case, however, their inclusion does not lead to a significant improvement in the structural precision (RMSD) since the original set of structures for the GTP class II aptamer was already calculated using a large number of NOE, hydrogen-bond, and torsion-angle restraints (for example, 25 NOE-based distance restraints per residue). However, when the structure calculations were repeated without torsion-angle restraints for residues in non-canonical elements, the inclusion of the newly observable NOEs involving previously invisible amino groups led to a significant improvement in structural precision (Supporting Information, Table S1 and Figure S7), presumably due to their long-range nature. Thus, the additional distance information obtained through the  $^{13}\text{C}$ -detected "amino"-NOESY experiment might be particularly valuable in cases where only a limited number of restraints is experimentally accessible. Furthermore, NOE contacts from amino groups can be a decisive factor in the structural characterization of larger systems with dynamic regions. In this case, often only very few NOE contacts are observable. This is particularly relevant when there are no imino proton signals due to fast exchange with water and therefore no information about the orientation of the respective nucleobase can be extracted.

In summary, we provide a set of experiments which enable the detailed structural characterization of RNA amino groups. With the C(N)H-HDQC experiment a complete set of amino group resonances can be detected for all three amino-group-bearing nucleotide types. The obtained chemical shift information enables discrimination between canonical and non-canonical base interactions in many cases. Furthermore, the reduced sensitivity of amino protons to chemical exchange with water<sup>[19]</sup> allows us to extract structural information about dynamic regions of RNA and also enables measurements over a wide temperature range. Compared to an imino proton-based characterization of base pairs, this is beneficial since amino groups are present in three of the four nucleotide types and do not require measurements at low temperatures. Besides chemical shift information, direct structural restraints from the "amino"-NOESY experiment can be exploited that cannot be observed otherwise. With these experiments, the amino protons succeed imino protons as the standard reporter signal for the characterization of base pair interactions in nucleic acids.

## Acknowledgements

Wolfgang Bermel is acknowledged for helpful discussions on H–N transfer methods. Nusrat Qureshi is acknowledged for insightful discussions. Furthermore, we acknowledge Katharina Weickhmann and Matthias Görlach for providing the 43 nt and 329 nt RNAs, respectively. Work at BMRZ is supported by the state of Hesse. R.S. is a recipient of a stipend of the Fonds der Chemischen Industrie. H.S., J.W., and B.F. are supported by the DFG in the collaborative research center 902, H.S. and B.F. are supported by the DFG in graduate school CLIC (GRK 1986).

## Conflict of interest

The authors declare no conflict of interest.

**Keywords:**  $^{13}\text{C}$  direct detection · double quantum · NMR spectroscopy · NOESY · RNA

**How to cite:** *Angew. Chem. Int. Ed.* **2019**, *58*, 9140–9144  
*Angew. Chem.* **2019**, *131*, 9238–9242

- [1] N. B. Leontis, J. Stombaugh, E. Westhof, *Nucleic Acids Res.* **2002**, *30*, 3497–3531.
- [2] H. Schwalbe, J. Buck, B. Fürtig, J. Noeske, J. Wöhnert, *Angew. Chem. Int. Ed.* **2007**, *46*, 1212–1219; *Angew. Chem.* **2007**, *119*, 1232–1240.
- [3] E. L. Ulrich, H. Akutsu, J. F. Doreleijers, Y. Harano, Y. E. Ioannidis, J. Lin, M. Livny, S. Mading, D. Maziuk, Z. Miller, et al., *Nucleic Acids Res.* **2008**, *36*, D402–D408.
- [4] R. Michalczuk, I. M. Russu, *Biophys. J.* **1999**, *76*, 2679–2686.
- [5] M. Adrian, F. R. Winnerdy, B. Heddi, A. T. Phan, *Biophys. J.* **2017**, *113*, 775–784.
- [6] L. D. Williams, N. G. Williams, B. R. Shaw, *J. Am. Chem. Soc.* **1990**, *112*, 829–833.
- [7] a) L. Mueller, P. Legault, A. Pardi, *J. Am. Chem. Soc.* **1995**, *117*, 11043–11048; b) F. A. A. Mulder, C. A. E. M. Spronk, M. Slijper, R. Kaptein, R. Boelens, *J. Biomol. NMR* **1996**, *8*, 223–228.
- [8] a) H. Jin, J. P. Loria, P. B. Moore, *Mol. Cell* **2007**, *26*, 205–215; b) B. Fürtig, C. Richter, W. Bermel, H. Schwalbe, *J. Biomol. NMR* **2004**, *28*, 69–79.
- [9] R. Fiala, V. Sklenár, *J. Biomol. NMR* **2007**, *39*, 153–163.
- [10] H. W. Mackenzie, D. F. Hansen, *J. Biomol. NMR* **2017**, *69*, 123–132.
- [11] G. A. Morris, R. Freeman, *J. Am. Chem. Soc.* **1979**, *101*, 760–762.
- [12] A. J. Shaka, C. J. Lee, A. Pines, *J. Magn. Reson.* **1988**, *77*, 274–293.
- [13] W. Bermel, I. Bertini, L. Duma, I. C. Felli, L. Emsley, R. Pierattelli, P. R. Vasos, *Angew. Chem. Int. Ed.* **2005**, *44*, 3089–3092; *Angew. Chem.* **2005**, *117*, 3149–3152.
- [14] S. Nozinovic, B. Fürtig, H. R. A. Jonker, C. Richter, H. Schwalbe, *Nucleic Acids Res.* **2010**, *38*, 683–694.
- [15] a) A. C. Wolter, E. Duchardt-Ferner, A. H. Nasiri, K. Hantke, C. H. Wunderlich, C. Kreutz, J. Wöhnert, *Biomol. NMR Assignments* **2016**, *10*, 101–105; b) A. C. Wolter, A. K. Weickhmann, A. H. Nasiri, K. Hantke, O. Ohlenschläger, C. H. Wunderlich, C. Kreutz, E. Duchardt-Ferner, J. Wöhnert, *Angew. Chem. Int. Ed.* **2017**, *56*, 401–404; *Angew. Chem.* **2017**, *129*, 412–415.
- [16] a) W. Bermel, I. Bertini, I. Felli, M. Piccioli, R. Pierattelli, *Prog. Nucl. Magn. Reson. Spectrosc.* **2006**, *48*, 25–45; b) B. Fürtig, R.

- Schnieders, C. Richter, H. Zetsche, S. Keyhani, C. Helmling, H. Kovacs, H. Schwalbe, *J. Biomol. NMR* **2016**, *64*, 207–221.
- [17] a) J. Leppert, C. R. Urbinati, S. Häfner, O. Ohlenschläger, M. S. Swanson, M. Görlach, R. Ramachandran, *Nucleic Acids Res.* **2004**, *32*, 1177–1183; b) K. Riedel, C. Herbst, S. Häfner, J. Leppert, O. Ohlenschläger, M. S. Swanson, M. Görlach, R. Ramachandran, *Angew. Chem. Int. Ed.* **2006**, *45*, 5620–5623; *Angew. Chem.* **2006**, *118*, 5748–5751.
- [18] N. B. Leontis, E. Westhof, *RNA* **2001**, *7*, 499–512.
- [19] A. Kettani, M. Gue, J. Leroy, *J. Am. Chem. Soc.* **1997**, *119*, 1108–1115.

Manuscript received: April 3, 2019  
Version of record online: May 27, 2019

---